INORGANIC CHEMISTRY
FRONTIERS

PAPER

A family of [Ni$_8$] cages templated by μ_6-peroxide from dioxygen activation†

Cite this: *Inorg. Chem. Front.*, 2014, **1**, 487

Alexandros Perivolaris,[a] Constantinos C. Stoumpos,[a] Jolanta Karpinska,[b] Alan G. Ryder,[b] Jamie M. Frost,[c] Kevin Mason,[c] Alessandro Prescimone,[c] Alexandra M. Z. Slawin,[d] Vadim G. Kessler,[e] Jennifer S. Mathieson,[f] Leroy Cronin,[f] Euan K. Brechin*[c] and Giannis S. Papaefstathiou*[a]

Received 2nd April 2014,
Accepted 12th May 2014

DOI: 10.1039/c4qi00048j

rsc.li/frontiers-inorganic

A family of exceptionally thermally stable [Ni$_8$] cages is reported, each being templated by a rare η^3:η^3:μ_6-O_2^{2-} species produced by dioxygen activation, where the reducing agent for the O_2 reduction appears to be the ligand used in the reaction mixtures, which was found within the nickel cages in its oxidized form.

Introduction

Dioxygen activation has provided substantial impetus for important developments in several different fields. These include biomimetic and bioinorganic chemistry which aim to reveal the structures of the reactive intermediates at the active sites of metalloenzymes and give insights into the mechanistic details of dioxygen activation and oxygenation reactions,[1–6] and catalysis since the metal–dioxygen intermediates have been proposed as active oxidants in C–H bond activation reactions.[3]

It has been proposed that dioxygen activation first involves bonding of dioxygen at a reduced metal center to form metal-superoxo or metal-peroxo intermediates, followed by O···O bond cleavage leading to the formation of high-valent, metal-oxo species, which are responsible for the oxidation reaction of the substrates within the metalloenzyme.[1–6] It is therefore believed that the presence of a redox-active metal center is a fundamental prerequisite for activating and reducing dioxygen.

Indeed, over the years, several high-valent metal-peroxo complexes, obtained by the action of dioxygen on a reduced metal center, have been structurally characterized by single-crystal X-ray crystallography.[4] Examples include Ti(IV)-peroxo,[4a] V(V)-peroxo,[4b] Cr(IV)-peroxo,[4c] Mn(III)-peroxo,[4d] Mn(IV)-peroxo,[4e] Fe(III)-peroxo,[4f] Co(III)-peroxo[4g–k] and Cu(II)-peroxo[4l,m] complexes that were isolated by the action of dioxygen on Ti$_2$(III), V(III), Cr(II), Mn(II), Mn(I), Fe(II), Co(II) and Cu(I) precursors, respectively.

Restricting further discussion to nickel–dioxygen species, there is only one Ni(II)-peroxo[5a] and one Ni(II)-superoxo[5b] compound, obtained by the oxygenation of a Ni^0 and a Ni^I precursor, respectively, which have been structurally characterized. There are also a few reports of spectroscopically characterized nickel-peroxo and nickel-superoxo complexes obtained by the action of dioxygen on low-valent Ni^0 and Ni^I precursors,[2e,3a,6] while there are no structurally characterized Ni(II)-peroxo species obtained by the action of dioxygen on Ni(II) centers.

Since Ni(II) is inert toward O_2, the most common approach to obtain Ni(II)-peroxo or Ni(II)-superoxo complexes is the use of H_2O_2.[5b] Indeed, there are a handful of structurally characterized Ni(II)-peroxo[7a,b] and Ni(II)-superoxo[7c,d] species obtained by the reaction of H_2O_2 with Ni(II) or Ni(III) precursors, respectively. It is worth noting that one Ni(II)-peroxo complex[8] has been obtained by the chemical reduction of a Ni(II)-superoxo precursor,[5b] with the latter being originally synthesized by the reaction of a Ni(I) precursor with O_2.

We herein report a family of [Ni$^{II}_8$] cages templated by a rare η^3:η^3:μ_6-O_2^{2-} species produced by dioxygen reduction. Although we cannot ignore the presence of the Ni(II) ions, which might indeed be involved in the dioxygen activation, the reducing agent for the O_2 reduction appears to be the ligand used in the reaction mixtures, which was found within the

[a]*Laboratory of Inorganic Chemistry, Department of Chemistry, National and Kapodistrian University of Athens, Panepistimiopolis, 157 71 Zografou, Greece. E-mail: gspapaef@chem.uoa.gr; Fax: +30 2107274782; Tel: +30 2107274840*
[b]*Nanoscale Biophotonics Laboratory, School of Chemistry, National University of Ireland, Galway, Ireland*
[c]*EaStCHEM School of Chemistry, The University of Edinburgh, West Mains Road, Edinburgh, EH9 3JJ, UK. E-mail: ebrechin@staffmail.ed.ac.uk; Fax: +44 (0)11 2754598; Tel: +44 (0)131 650 7545*
[d]*School of Chemistry, The University of St. Andrews, Purdie Building, St. Andrews, Fife KY16 9ST, UK*
[e]*Department of Chemistry, Swedish University of Agricultural Sciences, Box 7015, 750 07 Uppsala, Sweden*
[f]*WestCHEM, School of Chemistry, The University of Glasgow, University Avenue, Glasgow, G12 8QQ, UK*
†Electronic supplementary information (ESI) available: Supplementary figures. CCDC 894474–894477. For ESI and crystallographic data in CIF or other electronic format see DOI: 10.1039/c4qi00048j

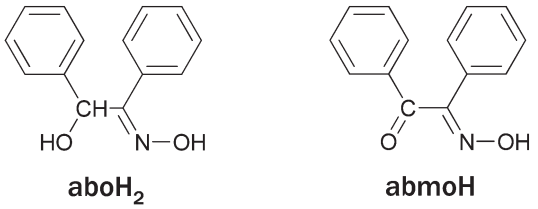

$aboH_2$ abmoH

Scheme 1 The structures of α-benzoin oxime ($aboH_2$) and α-benzilmonoxime (abmoH).

nickel cages in its oxidized form. Specifically, three octanuclear Ni(II) cages, namely $[Ni_8(O_2)(abmo)_6(MeCO_2)_2(MeO)_6(MeOH)_4]\cdot 4H_2O$ (**1**·$4H_2O$), $[Ni_8(O_2)(abmo)_6(PhCO_2)_2(MeO)_6(MeOH)_4]\cdot 2MeOH$ (**2**·2MeOH) and $[Ni_8(O_2)(abmo)_6(4ClPhCO_2)_2(MeO)_6(MeOH)_2(H_2O)_2]$ (**3**) (abmoH = α-benzilmonoxime, Scheme 1), were isolated from the reaction of nickel(II) carboxylates with α-benzoin oxime ($aboH_2$, Scheme 1) in MeOH under aerobic conditions. Interestingly, abmoH is the oxidized form of $aboH_2$. Direct evidence that the peroxide originates from the dioxygen reduction was provided by $^{18}O_2$ labelling experiments in a deoxygenated reaction mixture of **2**. To the best of our knowledge, complexes **1–3** represent the first examples of structurally characterized Ni(II)-peroxo complexes obtained by the action of dioxygen on Ni(II) precursors.

Such a dioxygen reduction where both the peroxide, O_2^{2-} (*i.e.* the reduced species), and the oxidized species (*i.e.* the $abmo^-$) are isolated and structurally characterized in the final product, and in which the metal ion appears not to change its oxidation state, has never been observed. This means that the electrons needed to reduce the dioxygen to O_2^{2-} are provided by the organic ligand (*i.e.* not the metal ion). The significance of these findings is the provision of evidence that the dioxygen activation and its subsequent reduction may also depend on the organic surroundings of the metal-containing active site of metalloenzymes.[1,2s–u] We note that there are reports of structurally characterized metal-peroxo complexes obtained by dioxygen reduction where the metal center does not change the oxidation state, but in all cases the reducing agent was not identified.[9] The same $[Ni_8]$ cages can be isolated from the reaction of nickel(II) carboxylates with abmoH, but only when H_2O_2 is added into the reaction mixtures. One side product, namely $[Ni_5(abo)_2(aboH)_6]\cdot 4MeOH\cdot CH_2Cl_2$ (**4**·4MeOH·CH_2Cl_2), was also isolated and characterized by X-ray crystallography. To the best of our knowledge, cages **1–3** represent the first polynuclear metal complexes which can be synthesized from different organic ligands (*i.e.* $aboH_2$ and abmoH).

Experimental section

Materials and methods

$Ni(MeCO_2)_2\cdot 4H_2O$, $aboH_2$ (α-benzoin oxime) H_2O_2, Et_3N, KBr, $^{18}O_2$ (90%, ^{18}O-enriched) and $H_2{}^{18}O_2$ (2–3% solution, 90% ^{18}O-enriched) and all solvents were purchased from commercial sources and used as received. $Ni(PhCO_2)_2\cdot 3H_2O$,[10] $Ni(4ClPhCO_2)_2$[10] ($4ClPhCO_2H$ = 4-chloro-benzoic acid) and abmoH[11] (α-benzilmonoxime) were prepared according to literature procedures. IR spectra were recorded as KBr pellets in the 4000–400 cm^{-1} range on a Shimadzu FT/IR IRAffinity-1 spectrometer. TGA data were collected with a Mettler Toledo TGA/DCS1 instrument in 40 μl Al pans under a N_2 flow of 50 ml min^{-1}. Small sample portions (~1–2 mg) were used to avoid damage to the instrument due to the explosive nature of the peroxide complexes. Variable-temperature, solid-state direct current (dc) magnetic susceptibility data down to 5 K were collected on a Quantum Design MPMS-XL SQUID magnetometer equipped with a 7 T dc magnet. Diamagnetic corrections were applied to the observed paramagnetic susceptibilities using Pascal's constants.

Raman spectroscopy

Raman spectra were collected for all samples on two different Raman spectrometers, both with 785 nm excitation. The first system was a Raman WorkStation™ (Kaiser Optical Systems Inc., Ann Arbor, MI) over a 200–3000 cm^{-1} spectral range, with a resolution of ~3–4 cm^{-1}. This system was equipped with a −40 °C cooled CCD detector. The second system was a RamanStation spectrometer (AVALON Instruments Ltd, Belfast) equipped with a TE cooled (−90 °C) back thinned CCD detector. A laser power of ~70 mW (at the sample) with an exposure time of 2 × 10 seconds was used and spectra were collected from 250 to 3311 cm^{-1} (at a resolution of 4 cm^{-1}). For all data, exposure times (between 10 and 45 seconds) and accumulation numbers were varied in order to attain the optimal signal to noise (S/N) ratio in the Raman spectra, so that any shifts in the peroxo bonds could be accurately measured. The spectra were not corrected for instrument response.

Mass spectrometry

Analysis was carried out using a Bruker Maxis Impact instrument with an electrospray (ESI-MS) ionisation source. The calibration solution used was an Agilent ESI-L low concentration tuning mix solution, Part No. G1969-85000, enabling calibration between approximately 50 *m*/*z* and 2000 *m*/*z*. Samples were dissolved in CH_2Cl_2/CH_3OH at concentrations of 10^{-4} mol L^{-1} and introduced into the MS at a dry gas temperature of 180 °C. The ion polarity for all MS scans recorded was positive, with the voltage of the capillary tip set at 4000 V, end plate offset at −500 V, funnel 1 RF at 400 Vpp and funnel 2 RF at 400 Vpp, hexapole RF at 200 Vpp, ion energy at 5 eV, collision energy at 5 eV, collision cell RF at 1500 Vpp, transfer time at 120.0 μs and the pre-pulse storage time at 10.0 μs. Each spectrum was collected for 2 min.

Synthesis

$[Ni_8(O_2)(abmo)_6(MeCO_2)_2(MeO)_6(MeOH)_4]\cdot 4H_2O$ (1·$4H_2O$) and $[Ni_5(abo)_2(aboH)_6]\cdot 4MeOH\cdot CH_2Cl_2$ (4·4MeOH·CH_2Cl_2) from $aboH_2$. To a slurry of $Ni(MeCO_2)_2\cdot 4H_2O$ (0.4 mmol) and $aboH_2$ (0.4 mmol) in MeOH (25 mL) was added a 1 M Et_3N solution in EtOH (0.8 mmol). The slurry was stirred for 4 hours, during which time an orange-yellow precipitate

formed in ~20% yield (based on Ni). The precipitate was filtered and the dark green-brown filtrate left undisturbed for 4 days. Dark green single crystals of **1**·4H_2O were formed in ~55% yield (based on Ni). The crystals were collected by vacuum filtration, washed with a small amount of MeOH and Et_2O, and dried in air. Recrystallization of the orange-yellow powder from CH_2Cl_2/MeOH afforded orange-yellow crystals of **4**·4MeOH·CH_2Cl_2. Elemental analysis for **1**·4H_2O (%) calcd for $C_{98}H_{108}N_6O_{32}Ni_8$: C 50.05, H 4.63, N 3.57; found: C 50.10, H 4.50, N 3.53. Elemental analysis for **4**·4MeOH·CH_2Cl_2 (%) calcd for $C_{117}H_{112}N_8O_{20}Cl_2Ni_5$: C 60.71, H 4.88, N 4.84; found: C 60.69, H 4.82, N 4.80. IR for **1**·4H_2O, cm^{-1} (KBr pellets): 3052 w, 2923 w, 2810 w, 1583 s, 1551 s, 1444 sh, 1407 s, 1344 s, 1286 s, 1268 s, 1194 s, 1176 s, 1098 w, 1052 m, 1025 s, 999 w, 917 s, 793 br, 745 m, 719 w, 696 sh, 680 m, 642 w, 618 w, 582 w, 439 br. IR for **4**·4MeOH·CH_2Cl_2, cm^{-1} (KBr pellets): 1705 br, 1492 sh, 1452 sh, 1444 sh, 1138 br, 1111 br, 1069 sh, 1042 w br 1018 w br, 917 w, 835 w.

$[Ni_8(O_2)(abmo)_6(PhCO_2)_2(MeO)_6(MeOH)_4]$·2MeOH (2·2MeOH) and $[Ni_8(O_2)(abmo)_6(4ClPhCO_2)_2(MeO)_6(MeOH)_2(H_2O)_2]$ (3) along with (4). These were prepared in a similar manner to the above synthesis, replacing $Ni(MeCO_2)_2$·4H_2O with $Ni(PhCO_2)_2$·3H_2O and $Ni(4ClPhCO_2)_2$, respectively. The relevant yields for **2**·2MeOH and **4** were 60% and 15%, respectively, while those for **3** and **4** were 65% and 12%, respectively. Elemental analysis for **2**·2MeOH (%) calcd for $C_{110}H_{112}N_6Ni_8O_{30}$: C 53.54, H 4.57, N 3.41; found: C 53.50, H 4.53, N 3.44. IR for **2**·2MeOH, cm^{-1} (KBr pellets): 3049 w, 2917 w, 2812 w, 1588 s, 1547 s, 1444 sh, 1393 s, 1345 s, 1286 s, 1268 s, 1194 s, 1176 s, 1099 w, 1051 m, 1024 s, 998 w, 916 s, 800 w, 746 m, 719 m, 696 sh, 679 m, 640 w, 620 w, 582 w, 434 br. Elemental analysis for **3** (%) calcd for $C_{106}H_{98}Cl_2N_6Ni_8O_{28}$: C 52.08, H 4.04, N 3.44; found: C 50.05, H 4.00, N 3.49. IR for **3**, cm^{-1} (KBr pellets): 3055 w, 2920 w, 2813 w, 1587 s, 1546 s, 1444 m, 1396 s, 1345 s, 1286 s, 1269 s, 1193 s, 1176 s, 1096 w, 1051 m, 1027 m, 998 w, 916 s, 798 w, 775 w, 746 m, 718 w, 696 sh, 688 w, 582 w, 439 br.

$[Ni_8(O_2)(abmo)_6(MeCO_2)_2(MeO)_6(MeOH)_4]$·4$H_2O$ (1·4H_2O) from abmoH. To a slurry of $Ni(MeCO_2)_2$·4H_2O (0.4 mmol) and abmoH (0.4 mmol) in MeOH (25 mL) were added H_2O_2 (30% solution, 0.4 mmol) and Et_3N (1 M solution in EtOH, 0.8 mmol). The slurry was stirred for 1 hour. The resulting dark green-brown solution was left undisturbed for 4 days. Dark green single crystals of **1**·4H_2O were formed in ~75% yield (based on Ni). The crystals were collected by vacuum filtration, washed with a small amount of MeOH and Et_2O and dried in air. Elemental analysis for **1**·4H_2O (%) calcd for $C_{98}H_{108}N_6O_{32}Ni_8$: C 50.05, H 4.63, N 3.57; found: C 50.12, H 4.53, N 3.52. IR for **1**·4H_2O, cm^{-1} (KBr pellets): 3052 w, 2923 w, 2810 w, 1583 s, 1551 s, 1444 sh, 1407 s, 1344 s, 1286 s, 1268 s, 1194 s, 1176 s, 1098 w, 1052 m, 1025 s, 999 w, 917 s, 793 br, 745 m, 719 w, 696 sh, 680 m, 642 w, 618 w, 582 w, 439 br.

$[Ni_8(O_2)(abmo)_6(PhCO_2)_2(MeO)_6(MeOH)_4]$·2MeOH (2·2MeOH) and $[Ni_8(O_2)(abmo)_6(4ClPhCO_2)_2(MeO)_6(MeOH)_2(H_2O)_2]$ (3). These were prepared in a similar manner to the above synthesis by replacing $Ni(MeCO_2)_2$·4H_2O with $Ni(PhCO_2)_2$·3H_2O and $Ni(4ClPhCO_2)_2$, respectively. The relevant yields for **2**·2MeOH and **3** were 77% and 79%, respectively. Elemental analysis for **2**·2MeOH (%) calcd for $C_{110}H_{112}N_6Ni_8O_{30}$: C 53.54, H 4.57, N 3.41; found: C 53.52, H 4.54, N 3.43. IR for **2**·2MeOH, cm^{-1} (KBr pellets): 3049 w, 2917 w, 2812 w, 1588 s, 1547 s, 1444 sh, 1393 s, 1345 s, 1286 s, 1268 s, 1194 s, 1176 s, 1099 w, 1051 m, 1024 s, 998 w, 916 s, 800 w, 746 m, 719 m, 696 sh, 679 m, 640 w, 620 w, 582 w, 434 br. Elemental analysis for **3** (%) calcd for $C_{106}H_{98}Cl_2N_6Ni_8O_{28}$: C 52.08, H 4.04, N 3.44; found: C 50.07, H 4.02, N 3.45. IR for **3**, cm^{-1} (KBr pellets): 3055 w, 2920 w, 2813 w, 1587 s, 1546 s, 1444 m, 1396 s, 1345 s, 1286 s, 1269 s, 1193 s, 1176 s, 1096 w, 1051 m, 1027 m, 998 w, 916 s, 798 w, 775 w, 746 m, 718 w, 696 sh, 688 w, 582 w, 439 br.

$[Ni_8(^{18}O_2)(abmo)_6(PhCO_2)_2(MeO)_6(MeOH)_4]$·2MeOH (2A·2MeOH) from aboH$_2$ and $^{18}O_2$. Manipulations were performed under argon in deoxygenated solvents using standard Schlenk techniques. To a slurry of $Ni(PhCO_2)_2$·3H_2O (0.4 mmol) and aboH$_2$ (0.4 mmol) in deoxygenated MeOH (25 mL) was added a 1 M Et_3N solution in EtOH (0.8 mmol). The slurry was stirred for 1 hour, during which time an orange-yellow precipitate formed in ~20% yield (based on Ni). The precipitate was filtered and the green filtrate bubbled with 250 mL of $^{18}O_2$ (90%, ^{18}O-enriched). The solution turned dark-green brown and was left undisturbed for 4 days. Dark green single crystals of **2A**·2MeOH were formed in ~63% yield (based on Ni). The crystals were collected by vacuum filtration, washed with a small amount of MeOH and Et_2O and dried in air. Analytical data as well as IR data were identical to those of **2**·2MeOH.

$[Ni_8(^{18}O_2)(abmo)_6(PhCO_2)_2(MeO)_6(MeOH)_4]$·2MeOH (2A·2MeOH) from abmoH and $H_2{}^{18}O_2$. To a slurry of $Ni(PhCO_2)_2$·3H_2O (0.4 mmol) and abmoH (0.4 mmol) in MeOH (25 mL) were added $H_2{}^{18}O_2$ (2–3% solution, 90% ^{18}O-enriched, 100 mg) and Et_3N (1 M solution in EtOH, 0.8 mmol). The slurry was stirred for 1 hour. The resulting dark green-brown solution was left undisturbed for 4 days. Dark green single crystals of **2A**·2MeOH were formed in ~70% yield (based on Ni). The crystals were collected by vacuum filtration, washed with a small amount of MeOH and Et_2O and dried in air. Analytical data as well as IR data were identical to those of **2**·2MeOH.

Results and discussion

Syntheses

The reaction of $Ni(MeCO_2)_2$·4H_2O with aboH$_2$ in MeOH and in the presence of triethylamine (Et_3N) at room temperature results in a yellow-orange powder and a dark green-brown solution. Recrystallization of the yellow-orange powder revealed the pentanuclear complex **4**, while slow evaporation of the dark green-brown solution afforded X-ray quality dark green crystals of **1**. Similar reactions involving $Ni(PhCO_2)_2$·3H_2O or $Ni(4ClPhCO_2)_2$ resulted in the same yellow-orange powder and X-ray quality dark green crystals of **2** and **3**, respectively. The identity of the products is independent of the metal to ligand ratio. Performing the same reactions at elevated temperatures

(*i.e.* above 50 °C) substantially reduces the yield of complex **4** and increases the yields of complexes **1–3**. With the structures of complexes **1–3** known, we repeated the same reactions in the absence of O_2: in this case only complex **4** forms and the solution does not turn dark green-brown, but retains its original green color. In order to provide direct evidence that the μ_6-O_2^{2-} originates from the reduction of dioxygen we synthesized the ^{18}O-labelled complex **2** (**2A**) by the action of $^{18}O_2$ in a de-oxygenated reaction mixture of **2**. The ^{18}O-labelled **2A** was obtained and characterized by Raman spectroscopy. However, none of the bands in the recorded spectra were clearly identified as being sensitive to isotopic substitution of the peroxide. We therefore also performed ESI-MS on both unlabelled **2** and ^{18}O-labelled **2A**, where we observed a 4 unit shift correlating to the labelling of both O-atoms of the peroxo ligand. Having established the presence of the abmo$^-$ ligands within the cages of **1–3**, we attempted to isolate these complexes starting from abmoH instead of aboH_2. The solution does not turn dark green-brown until H_2O_2 is added to the reaction mixture in each case. As in the Ni$(RCO_2)_2$–aboH_2–Et_3N reaction system, the reactions of Ni$(RCO_2)_2$ with abmoH and H_2O_2 in MeOH in the presence of Et_3N result in dark green-brown solutions from which complexes **1–3** were isolated and their structures were re-confirmed by single-crystal X-ray crystallography. The ^{18}O-labelled **2A** was also synthesized by adding $H_2{}^{18}O_2$ to a reaction mixture of Ni$(PhCO_2)_2{\cdot}3H_2O$–abmoH–Et_3N.

Description of structures

Although complexes **1–3**[12] are not isostructural, their molecular structures are very similar. A labelled picture of the representative complex **1**, whose structure will be discussed in detail, is shown in Fig. 1 (see ESI† for figures of complexes **2** and **3**).

Complex **1**[12] crystallizes in the triclinic space group $P\bar{1}$. The [Ni_8] cage is situated at a center of inversion and consists of a $Ni_6(O_2)$ core with staggered symmetry (D_{3d}). The six Ni^{II} ions are situated at the apices of a distorted octahedron, with the Ni···Ni separations ranging from 3.362 to 4.856 Å. The octahedron is doubly face-capped by the remaining two Ni^{II} ions (Ni4 and Ni4′). All Ni^{II} ions are in distorted octahedral geometries. Six abmo$^-$ ligands bridge the central Ni_6 core in a η^1:η^1:η^1:μ-fashion, with each abmo$^-$ ligand chelating to one Ni^{II} ion through the carbonyl O atom and the oximato N atom and bridging to another through the deprotonated oximato O atom. Six μ_3-MeO$^-$ ligands (three unique: O71, O72 and O73) bridge the peripheral, face-capping Ni^{II} ions to the central core. The octahedral environment around these peripheral Ni^{II} ions is completed by two MeOH molecules and a terminal $MeCO_2^-$ ligand. Alternatively, the metal core of the octanuclear cage may be described as being composed of two "corner" sharing cubanes, with the shared "corner" being the μ_6-O_2^{2-} moiety (Fig. 1). The presence of abmo$^-$ corroborates the absence of the hydrogen atom at the carbonyl carbon atom and the short C···O distance (*i.e.* 1.243(7), 1.246(7) and 1.253 (6) Å for each of the three abmo$^-$ ligands) and the presence of a C=O bond. The η^3:η^3:μ_6-O_2^{2-} is fully surrounded by (six) Ni^{II} ions at the very center of the cage, and clearly templates the formation of the octanuclear cluster. It would appear highly unlikely that the octanuclear metal cage would form first, before O_2^{2-} encapsulation. The O–O bond length in the peroxide is 1.487(4) Å [1.508 Å in **2**[12] and 1.491 Å in **3**[12]] and is well within the limits of other reported peroxide bond lengths.[1–9] The Ni–$O_{peroxide}$ bond lengths are 2.055(3) Å, 2.031(3) Å and 2.015(3) Å for Ni1–O81, Ni2–O81 and Ni3–O81, respectively, with the Ni–$O_{peroxide}$–Ni angles being 114.61(13)°, 97.58(12)° and 113.09(13)° for the Ni1–O81–Ni2, Ni1–O81–Ni3 and Ni2–O81–Ni3 angles, respectively. The Ni–O81–O81′ angles are 111.47(19)°, 108.76(18)° and 111.03(19)° for Ni1, Ni2 and Ni3, respectively.

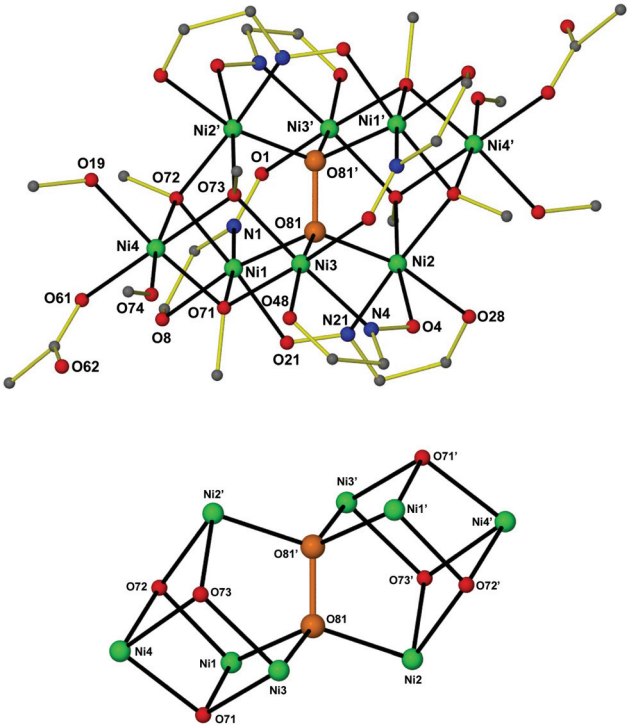

Fig. 1 The structure of [$Ni_8(O_2)$(abmo)$_6$($MeCO_2$)$_2$(MeO)$_6$($MeOH$)$_4$] **1** (top). All hydrogen atoms and most carbon atoms have been omitted for clarity. A view of the metal–oxygen core (bottom). Only the metal ions, the peroxide and the methoxide oxygen atoms are shown. Colour code: Ni green, C grey, N blue, O red. The η^3:η^3:μ_6-O_2^{2-} has been highlighted in orange. Symmetry code: (′) $-x$, $1-y$, $-z$.

Complexes **1–3** join a handful of structurally characterized abmoH complexes[13] and a very limited number of structurally characterized Ni^{II}-peroxo complexes.[5a,7a,b,8] Indeed the related complex [$Ni_8(O_2)(L)_{12}$][NO_3)$_2$ (**5**; LH = N-substituted 3-hydroxy-2-pyridinone) is the only other reported example containing the η^3:η^3:μ_6-O_2^{2-} ion.[7a] The formation of the latter cluster was achieved only when H_2O_2 was added into the reaction mixture. The central $Ni_6(O_2)$ core in **5** is similar to that seen for **1–3**, but with the two capping Ni^{II} ions residing in the faces of the octahedron lying in the same plane as the O_2^{2-} ion, rather than in the perpendicular plane for **1–3**. Other dissimilarities are the

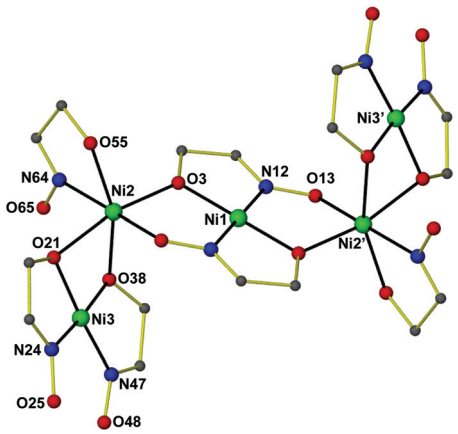

Fig. 2 The structure of $[Ni_5(abo)_2(aboH)_6]$ **4**. All hydrogen atoms and most carbon atoms have been omitted for clarity. Color code: Ni green, C grey, N blue, O red. Symmetry code: (′) 1 – *x*, –*y*, 1 – *z*.

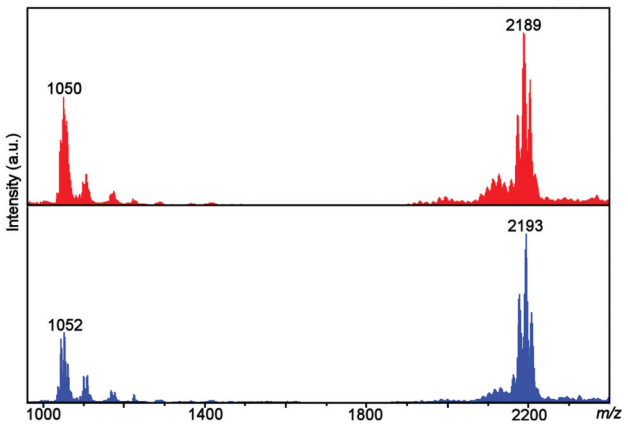

Fig. 3 ESI-MS of **2** (top, red) and **2A** (bottom, blue) showing the observation of the unlabelled and ^{18}O labelled $[Ni_8]$ complexes.

square pyramidal coordination geometry around the central Ni^{II} atoms and the absence of the MeO^- bridges.

Complex **4**[12] (Fig. 2) crystallizes in the triclinic space group $P\bar{1}$. The $[Ni_5]$ cluster is situated at an inversion center and consists of five coplanar Ni^{II} atoms, two abo^{2-} and six $aboH^-$ ligands. The central Ni^{II} atom (Ni1) is in a square planar geometry, being chelated by the hydroxyl oxygen atoms and oximato nitrogen atoms from two $\eta^2{:}\eta^1{:}\eta^1{:}\mu_3$ abo^- ligands in a *trans* conformation. The hydroxyl O atom and the oximato O atom from both sides of the central Ni1 bridge Ni2 and its symmetry equivalent ion. Ni2 is in a distorted octahedral environment, being surrounded by a chelating $aboH^-$ ligand and the hydroxyl oxygen atoms from a *cis*-$[Ni(aboH)_2]$ subunit. The latter consists of a square planar Ni^{II} ion (Ni3) being chelated by two $\eta^1{:}\eta^2{:}\mu$ $aboH^-$ ligands through the hydroxyl oxygen atoms and the oximic nitrogen atoms in a *cis* configuration. Complex **4** is one of just a few structurally characterized $aboH_2$ complexes.[14]

Raman spectroscopy

Raman spectra, for the comparison of the ^{16}O (**2**·2MeOH) and ^{18}O (**2A**·2MeOH) complexes, were collected for all samples on two different Raman spectrometers, both with 785 nm excitation. Although we used two different Raman spectrometers and varied both the exposure times and accumulation numbers in order to maximize the signal to noise (S/N) ratio in the Raman spectra, we did not observe any shifts in the respective spectra that could be ascribed conclusively to the peroxide stretching mode (Fig. S3 and S4 in the ESI†). Moreover, no Raman band was found to be sensitive to isotopic substitution with ^{18}O in the known $[Ni_8(O_2)(L)_{12}](NO_3)_2$ cluster.[7a] It should be noted that the Raman spectra were relatively noisy and if a weak peroxide band was present it was most likely buried in the noise signal.

Mass spectrometry

Both the unlabelled (**2**) and ^{18}O-labelled (**2A**) complexes were observed as both 1+ and 2+ species where one or both benzoate ligands were lost. A shift of 4 units was observed in the spectrum of **2A** compared to the spectrum of **2**, with this shift correlating to the labelling of both O atoms of the peroxo ligand (see Fig. 3 and Tables 1 and 2 for mass spectra and assignments).

Table 1 Assigned formulae for the unlabelled complex **2**

m/*z*	Formula
1034	$[Ni_8(O_2)(abmo)_6(MeO)_6(H_2O)_2]^{2+}$
1041	$[Ni_8(O_2)(abmo)_6(MeO)_6(H_2O)(MeOH)]^{2+}$
1050	$[Ni_8(O_2)(abmo)_6(MeO)_6(H_2O)_2(MeOH)]^{2+}$
1059	$[Ni_8(O_2)(abmo)_6(MeO)_6(H_2O)_3(MeOH)]^{2+}$
2171	$[Ni_8(O_2)(abmo)_6(PhCO_2)(MeO)_6(H_2O)]^{+}$
2189	$[Ni_8(O_2)(abmo)_6(PhCO_2)(MeO)_6(H_2O)_2]^{+}$
2203	$[Ni_8(O_2)(abmo)_6(PhCO_2)(MeO)_6(H_2O)(MeOH)]^{+}$

Table 2 Assigned formulae for the ^{18}O-labelled complex **2A**

m/*z*	Formula
1043	$[Ni_8(^{18}O_2)(abmo)_6(MeO)_6(H_2O)(MeOH)]^{2+}$
1052	$[Ni_8(^{18}O_2)(abmo)_6(MeO)_6(H_2O)_2(MeOH)]^{2+}$
1061	$[Ni_8(^{18}O_2)(abmo)_6(MeO)_6(H_2O)_3(MeOH)]^{2+}$
2175	$[Ni_8(^{18}O_2)(abmo)_6(PhCO_2)(MeO)_6(H_2O)]^{+}$
2193	$[Ni_8(^{18}O_2)(abmo)_6(PhCO_2)(MeO)_6(H_2O)_2]^{+}$
2207	$[Ni_8(^{18}O_2)(abmo)_6(PhCO_2)(MeO)_6(H_2O)(MeOH)]^{+}$

Magnetic properties

Variable-temperature magnetic susceptibility data for the representative cage **1** were recorded between 250 and 5 K in an applied field of 1.0 kG. A plot of $\chi_M T$ *versus* T for **1** is shown in Fig. 4. The $\chi_M T$ product for complex **1** decreases upon cooling from a value of 7.88 cm^3 K mol^{-1} at 250 K to a value of 0.76 cm^3 K mol^{-1} at 5 K. The shape of the curve as well as the low value of the $\chi_M T$ product at 5 K suggest the presence of dominant antiferromagnetic exchange interactions and a diamagnetic spin ground state. The structural complexity of the

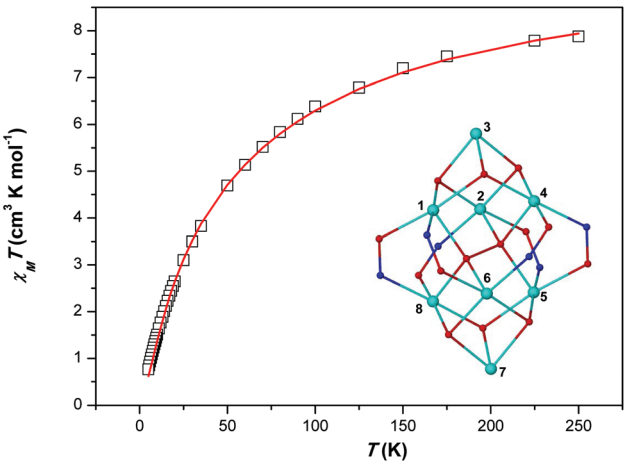

Fig. 4 $\chi_M T$ *vs.* T (□) plot for complex **1**. The solid red line represents the fit of the experimental data to spin-Hamiltonian (1) and the model shown in the inset – see text for details.

molecule (there are many different exchange interaction pathways present) precludes any detailed quantitative analysis. However, in order to qualitatively estimate the magnitude of the exchange, the experimental data were satisfactorily fitted using a simple one exchange parameter (J) model by employing spin Hamiltonian (1). The best fit parameter was $J = -5.02$ cm^{-1} with a fixed $g = 2.20$.

$$\begin{aligned}\hat{H} = &-2J(\hat{S}_1\cdot\hat{S}_2+\hat{S}_1\cdot\hat{S}_3+\hat{S}_1\cdot\hat{S}_4+\hat{S}_1\cdot\hat{S}_5+\hat{S}_1\cdot\hat{S}_6\\&+\hat{S}_1\cdot\hat{S}_8+\hat{S}_2\cdot\hat{S}_3+\hat{S}_2\cdot\hat{S}_4+\hat{S}_2\cdot\hat{S}_5+\hat{S}_2\cdot\hat{S}_6+\hat{S}_2\cdot\hat{S}_8\\&+\hat{S}_3\cdot\hat{S}_4+\hat{S}_4\cdot\hat{S}_5+\hat{S}_4\cdot\hat{S}_6+\hat{S}_4\cdot\hat{S}_8+\hat{S}_5\cdot\hat{S}_6+\hat{S}_5\cdot\hat{S}_7\\&+\hat{S}_5\cdot\hat{S}_8+\hat{S}_6\cdot\hat{S}_7+\hat{S}_6\cdot\hat{S}_8+\hat{S}_7\cdot\hat{S}_8)\end{aligned} \quad (1)$$

Thermal properties

Complexes **1–3** are stable in the solid state, can be handled in air and stored at room temperature as powdered samples or as single-crystals within their mother liquor for a period of over two years. Thermogravimetric analysis (TGA, Fig. 5) reveals that the three [Ni_8] cages are stable up to 200 °C. This is an abnormal behaviour for peroxide complexes[7a] and is attributed to the isolation of the μ_6-O_2^{2-} within the cores of the [Ni_8] cages.[15]

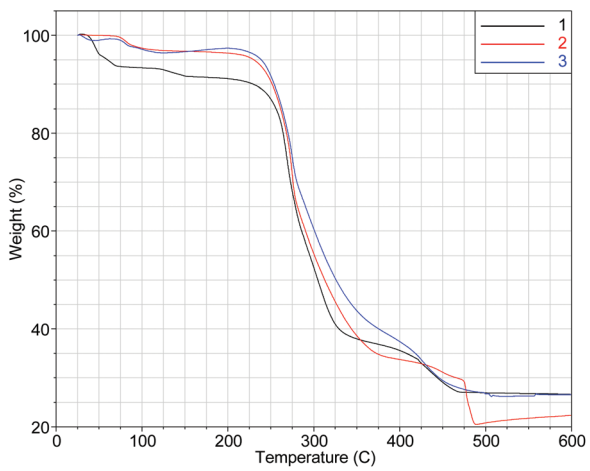

Fig. 5 TGA plots in the 25–600 °C range of **1–3**.

Conclusions

In summary, we have reported the synthesis and X-ray characterization of a family of octanuclear Ni^{II} cages which are templated by a rare η^3:η^3:μ_6-O_2^{2-} species produced by dioxygen activation. This is the first time the O_2^{2-} (*i.e.* the reduced species) and the reducing agent for the O_2 reduction – which is not the metal ion (*i.e.* the organic ligand found within the nickel cages in its oxidized form) – were isolated and characterized by X-ray crystallography within the same compound(s). Cages **1–3** also represent unique paradigms of O_2 activation and reduction by Ni^{II} reaction blends, which means that the electrons needed for reducing the dioxygen into the O_2^{2-} are not provided by the metal ion but by the organic ligand[2s–u] (*i.e.* $aboH_2$) which was found in its oxidized form (*i.e.* abmoH) within the cages. An alternative route providing access to the same [Ni_8] cages involves the use of the oxidized form of the ligand (*i.e.* abmoH) along with H_2O_2. The octanuclear cages are the first examples of polynuclear metal complexes which can be made from different organic ligands (*i.e.* $aboH_2$ and abmoH), and are exceptionally thermally stable (up to 200 °C).[15] They also increase the number of structurally characterized Ni^{II}-peroxo compounds from four[5a,7a,b,8] to seven. The vibrational modes of the μ_6-O_2^{2-} were not identified by Raman spectroscopy since no band was sensitive to isotopic substitution with ^{18}O; similarly no Raman band was found to be sensitive to isotopic substitution with ^{18}O in the known [Ni_8-(μ_6-O_2)$(L)_{12}$]$(NO_3)_2$ cluster.[7a] In contrast, a shift of 4 units was observed in the ESI-MS spectrum of the ^{18}O-labelled **2A** compared to the spectrum of unlabelled **2**. This shift correlates to the labelling of both O atoms of the peroxo ligand, thus providing direct evidence that the peroxide originates from the reduction of dioxygen. Magnetic susceptibility revealed relatively weak antiferromagnetic exchange interactions between neighboring Ni^{II} ions, resulting in a diamagnetic spin ground state. The side product, a [Ni_5] cluster, was also isolated and characterized by X-ray crystallography. We are currently exploring the coordination chemistry of $aboH_2$ and abmoH with other 3d and 4f ions while examining the chemical reactivity of the [Ni_8] cages.

Acknowledgements

This research has been co-financed by the European Union (European Social Fund – ESF) and Greek national funds through the Operational Program "Education and Lifelong Learning" of the National Strategic Reference Framework (NSRF) – the Research Funding Program: "THALES. Investing in knowledge society" through the European Social Fund.

The Bodossaki Foundation is also acknowledged for donating the TGA instrument to the Dept. of Chemistry of UoA.

Notes and references

1 (*a*) For a special issue on dioxygen activation by metalloenzymes and models, see: W. Nam (ed.), *Acc. Chem. Res*., 2007, **40**, 465–634; (*b*) For a forum on dioxygen activation and reduction, see: W. B. Tolman and E. I. Solomon, *Inorg. Chem.*, 2010, **49**, 3555–3556.

2 (*a*) J. S. Valentine, *Chem. Rev.*, 1973, **73**, 235–245; (*b*) L. Vaska, *Acc. Chem. Res.*, 1976, **9**, 175–183; (*c*) J. Reim, R. Werner, W. Haase and B. Krebs, *Chem. – Eur. J.*, 1998, **4**, 289–298; (*d*) C. J. Cramer, W. B. Tolman, K. H. Theopold and A. L. Rheingold, *Proc. Natl. Acad. Sci. U. S. A.*, 2003, **100**, 3635–3640; (*e*) M. T. Kieber-Emmons, R. Schenker, G. P. Yap, T. C. Brunold and C. G. Riordan, *Angew. Chem., Int. Ed.*, 2004, **43**, 6716–6718; (*f*) S. Hikichi, H. Okuda, Y. Ohzu and M. Akita, *Angew. Chem., Int. Ed.*, 2009, **48**, 188–191; (*g*) J. G. Liu, T. Ohta, S. Yamaguchi, T. Ogura, S. Sakamoto, Y. Maeda and Y. Naruta, *Angew. Chem., Int. Ed.*, 2009, **48**, 9262–9267; (*h*) P. L. Holland, *Dalton Trans.*, 2010, **39**, 5415–5425; (*i*) R. Sarangi, J. Cho, W. Nam and E. I. Solomon, *Inorg. Chem.*, 2011, **50**, 614–620; (*j*) S. Yao, C. Herwig, Y. Xiong, A. Company, E. Bill, C. Limberg and M. Driess, *Angew. Chem., Int. Ed.*, 2010, **49**, 7054–7058; (*k*) A. D. Bochevarov, J. Li, W. J. Song, R. A. Friesner and S. J. Lippard, *J. Am. Chem. Soc.*, 2011, **133**, 7384–7397; (*l*) J. Cho, S. Jeon, S. A. Wilson, L. V. Liu, E. A. Kang, J. J. Braymer, M. H. Lim, B. Hedman, K. O. Hodgson, J. S. Valentine, E. I. Solomon and W. Nam, *Nature*, 2011, **478**, 502–505; (*m*) Y. J. Park, J. W. Ziller and A. S. Borovik, *J. Am. Chem. Soc.*, 2011, **133**, 9258–9261; (*n*) E. I. Solomon, J. W. Ginsbach, D. E. Heppner, M. T. Kieber-Emmons, C. H. Kjaergaard, P. J. Smeets, L. Tian and J. S. Woertink, *Faraday Discuss.*, 2011, **148**, 11; (*o*) C. E. Tinberg and S. J. Lippard, *Acc. Chem. Res.*, 2011, **44**, 280–288; (*p*) L. Boisvert and K. I. Goldberg, *Acc. Chem. Res.*, 2012, **45**, 899–910; (*q*) S. Maji, J. C. Lee, Y. J. Lu, C. L. Chen, M. C. Hung, P. P. Chen, S. S. Yu and S. I. Chan, *Chem. – Eur. J.*, 2012, **18**, 3955–3968; (*r*) S. Yao and M. Driess, *Acc. Chem. Res.*, 2012, **45**, 276–287; (*s*) G. Dong, S. Shaik and W. Lai, *Chem. Sci.*, 2013, **4**, 3624–3635; (*t*) G. Dong and W. Lai, *J. Phys. Chem. B*, 2014, **118**, 1791–1798; (*u*) A. J. Fielding, J. D. Lipscomb and L. Que, *J. Biol. Inorg. Chem.*, 2014, DOI: 10.1007/s00775-014-1122-9, in press.

3 (*a*) R. Latifi, L. Tahsini, D. Kumar, G. N. Sastry, W. Nam and S. P. de Visser, *Chem. Commun.*, 2011, **47**, 10674–10676; (*b*) M. Zhou and R. H. Crabtree, *Chem. Soc. Rev.*, 2011, **40**, 1875–1884; (*c*) Y. Xiong, S. Yao, R. Muller, M. Kaupp and M. Driess, *Nat. Chem.*, 2010, **2**, 577–580; (*d*) C. Citek, C. T. Lyons, E. C. Wasinger and T. D. Stack, *Nat. Chem.*, 2012, **4**, 317–322; (*e*) L. M. Mirica, M. Vance, D. J. Rudd, B. Hedman, K. O. Hodgson, E. I. Solomon and T. D. Stack, *Science*, 2005, **308**, 1890–1892; (*f*) J. Reedijk, *Science*, 2005, **308**, 1876–1877; (*g*) M. Rolff, J. N. Hamann and F. Tuczek, *Angew. Chem., Int. Ed.*, 2011, **50**, 6924–6927.

4 (*a*) P. Jeske, G. Haselhorst, T. Weyhermueller, K. Wieghardt and B. Nuber, *Inorg. Chem.*, 1994, **33**, 2462–2471; (*b*) A. F. Cozzolino, D. Tofan, C. C. Cummins, M. Temprado, T. D. Palluccio, E. V. Rybak-Akimova, S. Majumdar, X. Cai, B. Captain and C. D. Hoff, *J. Am. Chem. Soc.*, 2012, **134**, 18249–18252; (*c*) A. Yokoyama, J. Eun Han, J. Cho, M. Kubo, T. Ogura, M. A. Siegler, K. D. Karlin and W. Nam, *J. Am. Chem. Soc.*, 2012, **134**, 15269–15272; (*d*) M. K. Coggins, X. Sun, Y. Kwak, E. I. Solomon, E. Rybak-Akimova and J. A. Kovacs, *J. Am. Chem. Soc.*, 2013, **135**, 5631–5640; (*e*) C.-M. Lee, C.-H. Chuo, C.-H. Chen, C.-C. Hu, M.-H. Chiang, Y.-J. Tseng, C.-H. Hu and G.-H. Lee, *Angew. Chem., Int. Ed.*, 2012, **51**, 5427–5430; (*f*) K. Kim and S. J. Lippard, *J. Am. Chem. Soc.*, 1996, **118**, 4914–4915; (*g*) E. Bouwman and W. L. Driessen, *J. Am. Chem. Soc.*, 1988, **110**, 4440–4441; (*h*) S. Schmidt, F. W. Heinemann and A. Grohmann, *Eur. J. Inorg. Chem.*, 2000, 1657–1667; (*i*) A. L. Gavrilova, C. Jin Qin, R. D. Sommer, A. L. Rheingold and B. Bosnich, *J. Am. Chem. Soc.*, 2002, **124**, 1714–1722; (*j*) D. B. Leznoff, M. J. Katz, L. K. L. Cheng, N. D. Draper and R. J. Batchelor, *J. Mol. Struct.*, 2006, **796**, 223–229; (*k*) G. Givaja, M. Volpe, M. A. Edwards, A. J. Blake, C. Wilson, M. Schröder and J. B. Love, *Angew. Chem., Int. Ed.*, 2007, **46**, 584–586; (*l*) M. Kodera, K. Katayama, Y. Tachi, K. Kano, S. Hirota, S. Fujinami and M. Suzuki, *J. Am. Chem. Soc.*, 1999, **121**, 11006–11007; (*m*) F. Meyer and H. Pritzkow, *Angew. Chem., Int. Ed.*, 2000, **39**, 2112–2115.

5 (*a*) M. Matsumoto and K. Nakatsu, *Acta Crystallogr., Sect. B: Struct. Crystallogr. Cryst.Chem.*, 1975, **31**, 2711–2713; (*b*) S. Yao, E. Bill, C. Milsmann, K. Wieghardt and M. Driess, *Angew. Chem., Int. Ed.*, 2008, **47**, 7110–7113.

6 (*a*) G. Wilke, H. Schott and P. Heimbach, *Angew. Chem., Int. Ed. Engl.*, 1967, **6**, 92–93; (*b*) S. Otsuka, A. Nakamura and Y. Tatsuno, *J. Am. Chem. Soc.*, 1969, **91**, 6994–6999; (*c*) K. Fujita, R. Schenker, W. Gu, T. C. Brunold, S. P. Cramer and C. G. Riordan, *Inorg. Chem.*, 2004, **43**, 3324–3326; (*d*) M. T. Kieber-Emmons, J. Annaraj, M. Sook Seo, K. M. Van Heuvelen, T. Tosha, T. Kitagawa, T. C. Brunold, W. Nam and C. G. Riordan, *J. Am. Chem. Soc.*, 2006, **128**, 14230–14231; (*e*) M. T. Kieber-Emmons and C. G. Riordan, *Acc. Chem. Res.*, 2007, **40**, 618–625; (*f*) A. Company, S. Yao, K. Ray and M. Driess, *Chem. – Eur. J.*, 2010, **16**, 9669–9675.

7 (*a*) E. J. Brown, A. K. Duhme-Klair, M. I. Elliott, J. E. Thomas-Oates, P. L. Timmins and P. H. Walton, *Angew. Chem., Int. Ed.*, 2005, **44**, 1392–1395; (*b*) J. Cho, R. Sarangi, J. Annaraj, S. Y. Kim, M. Kubo, T. Ogura, E. I. Solomon and W. Nam, *Nat. Chem.*, 2009, **1**, 568–572; (*c*) K. Shiren, S. Ogo, S. Fujinami, H. Hayashi, M. Suzuki, A. Uehara, Y. Watanabe and Y. Moro-oka, *J. Am. Chem. Soc.*, 2000, **122**, 254–262; (*d*) J. Cho, H. Furutachi, S. Fujinami, T. Tosha, H. Ohtsu, O. Ikeda, A. Suzuki, M. Nomura,

T. Uruga, H. Tanida, T. Kawai, K. Tanaka, T. Kitagawa and M. Suzuki, *Inorg. Chem.*, 2000, **46**, 2873–2885.

8 S. Yao, Y. Xiong, M. Vogt, H. Grutzmacher, C. Herwig, C. Limberg and M. Driess, *Angew. Chem., Int. Ed.*, 2009, **48**, 8107–8110.

9 (*a*) J. Auld, A. C. Jones, A. B. Leese, B. Cockayne, P. J. Wright, P. O'Brien and M. Motevalli, *J. Mater. Chem.*, 1993, **3**, 1203–1208; (*b*) N. Hovnaninian, J. Galloy and P. Miele, *Polyhedron*, 1995, **14**, 297–300; (*c*) A. Sofetis, F. Fotopoulou, C. P. Raptopoulou, Th. F. Zafiropoulos, S. P. Perlepes and N. Klouras, *Polyhedron*, 2009, **28**, 3356–3360; (*d*) E. I. Tolis, M. Helliwell, S. Langley, J. Raftery and R. E. P. Winpenny, *Angew. Chem., Int. Ed.*, 2003, **42**, 3804–3808.

10 J. Catterick and P. Thornton, *J. Chem. Soc., Dalton Trans.*, 1975, 233–238.

11 T. W. J. Taylor and M. S. Marks, *J. Chem. Soc.*, 1930, 2302–2307.

12 Crystal data for **1**·4H_2O: $C_{98}H_{108}N_6Ni_8O_{32}$, M = 2351.58, triclinic, a = 13.291(2) Å, b = 13.838(2) Å, c = 16.545(4) Å, α = 108.734(3)°, β = 105.788(3)°, γ = 101.737(2)°, V = 2628.1(8) Å^3, T = 293(2) K, space group $P\bar{1}$, Z = 1, MoKα, 17 894 reflections measured, 11 581 independent reflections (R_{int} = 0.0352). The final R_1 values were 0.0542 ($I > 2\sigma(I)$). The final w$R(F^2)$ values were 0.1391 ($I > 2\sigma(I)$). The final R_1 values were 0.0933 (all data). The final w$R(F^2)$ values were 0.1603 (all data). The goodness of fit on F^2 was 1.015. CCDC 894474. Crystal data for **2**·2MeOH: $C_{110}H_{112}N_6Ni_8O_{30}$, M = 2467.74, monoclinic, a = 13.259(2) Å, b = 28.761(5) Å, c = 15.273(3) Å, α = 90.00°, β = 103.829(2)°, γ = 90.00°, V = 5655.0(16) Å^3, T = 296(2) K, space group $P2(1)/c$, Z = 2, MoKα, 21 909 reflections measured, 8862 independent reflections (R_{int} = 0.0920). The final R_1 values were 0.0631 ($I > 2\sigma(I)$). The final w$R(F^2)$ values were 0.1463 ($I > 2\sigma(I)$). The final R_1 values were 0.1197 (all data). The final w$R(F^2)$ values were 0.1743 (all data). The goodness of fit on F^2 was 0.996. CCDC 894475. Crystal data for **3**: $C_{106}H_{98}Cl_2N_6Ni_8O_{28}$, M = 2444.48, triclinic, a = 13.372(10) Å, b = 14.701(11) Å, c = 15.110(11) Å, α = 94.446(6)°, β = 108.768(13)°, γ = 104.964(10)°, V = 2675(3) Å^3, T = 93(2) K, space group $P\bar{1}$, Z = 1, MoKα, 26 876 reflections measured, 9695 independent reflections (R_{int} = 0.0381). The final R_1 values were 0.0601 ($I > 2\sigma(I)$). The final w$R(F^2)$ values were 0.1644 ($I > 2\sigma(I)$). The final R_1 values were 0.0623 (all data). The final w$R(F^2)$ values were 0.1669 (all data). The goodness of fit on F^2 was 1.075. CCDC 894476. Crystal data for **4**·4MeOH·CH_2Cl_2: $C_{117}H_{112}Cl_2N_8Ni_5O_{20}$, M = 2314.67, triclinic, a = 12.8976(6) Å, b = 13.0924(6) Å, c = 16.4651(6) Å, α = 98.686(3)°, β = 99.661(3)°, γ = 90.904(3)°, V = 2707.0(2) Å^3, T = 150.0 K, space group $P\bar{1}$, Z = 1, Cu Kα, 54 794 reflections measured, 9656 independent reflections (R_{int} = 0.0484). The final R_1 values were 0.0686 ($I > 2\sigma(I)$). The final w$R(F^2)$ values were 0.1827 ($I > 2\sigma(I)$). The final R_1 values were 0.0829 (all data). The final w$R(F^2)$ values were 0.2087 (all data). The goodness of fit on F^2 was 0.9640. CCDC 894477.

13 (*a*) V. V. Sharutin, O. V. Molokova, O. K. Sharutina, T. I. Akimova, A. V. Gerasimenko and M. A. Pushilin, *Russ. J. Coord. Chem.*, 2004, **30**, 559–565; (*b*) E. Soleimani, *Rev. Chim.*, 2009, **60**, 484–487.

14 (*a*) G. Karotsis, C. Stoumpos, A. Collins, F. White, S. Parsons, A. M. Slawin, G. S. Papaefstathiou and E. K. Brechin, *Dalton Trans.*, 2009, 3388–3390; (*b*) E. S. Koumousi, M. J. Manos, C. Lampropoulos, A. J. Tasiopoulos, W. Wernsdorfer, G. Christou and T. C. Stamatatos, *Inorg. Chem.*, 2010, **49**, 3077–3079; (*c*) S. Liu, H. Zhu and J. Zubieta, *Polyhedron*, 1989, **8**, 2473–2480; (*d*) T. C. Stamatatos, G. Vlahopoulou, C. P. Raptopoulou, V. Psycharis, A. Escuer, G. Christou and S. P. Perlepes, *Eur. J. Inorg. Chem.*, 2012, 3121–3131; (*e*) G. C. Vlahopoulou, T. C. Stamatatos, V. Psycharis, S. P. Perlepes and G. Christou, *Dalton Trans.*, 2009, 3646–3649.

15 N. Lopez, D. J. Graham, R. McGuire Jr., G. E. Alliger, Y. Shao-Horn, C. C. Cummins and D. G. Nocera, *Science*, 2012, **335**, 450–453.

